W. M. Toscano[1]
Research Associate. Assoc. Mem. ASME

E. G. Cravalho
Assoc. Professor. Mem. ASME

Cryogenic Engineering Laboratory, Department of Mechanical Engineering, Massachusetts Institute of Technology, Cambridge, Mass.

O. M. Silvares
Asst. Professor, Escola Politecnica da Universidade de Sao Paulo, Caixa Postal 8174, Sao Paulo, Brazil. Assoc. Mem. ASME

C. E. Huggins
Assoc. Professor of Surgery, Harvard Medical School: Chief, Low Temperature Surgical Unit and Director, Blood Bank and Transfusion Service, Massachusetts General Hospital, Boston, Mass.

The Thermodynamics of Intracellular Ice Nucleation in the Freezing of Erythrocytes

A theoretical model describing the thermodynamics of intracellular ice nucleation is developed for red blood cells as a model biomaterial. Analytical expressions based on current theories of ice nucleation by both homogeneous and heterogeneous nucleation processes are coupled with a thermodynamic model for the loss of intracellular water during freezing. Numerical solutions for both modes of nucleation identify two cooling regions—high cooling rates and low cooling rates—separated by a sharp demarcation zone. The nucleation temperature for high cooling rates is approximately 20°K higher than the nucleation temperature for low cooling rates and is essentially independent of cooling rate in each region. The nucleation temperatures for heterogeneous nucleation are approximately 30°K higher than the nucleation temperatures for homogeneous nucleation in the two regions. For the case of heterogeneous nucleation, it is possible to increase the nucleation temperature by packing of catalysts via the concentration polarization effect. If the cell suspension is allowed to supercool before nucleation occurs in the extracellular medium, the sharp transition from low cooling rates to high cooling rates for heterogeneous nucleation shifts to much lower cooling rates. The dependence of the transition cooling rate on the degree of supercooling has been established for a typical freezing situation.

Introduction

The possibility of maintaining biomaterials in a state of suspended animation by freezing has intrigued man for centuries. Recent developments in the frozen preservation of human erythrocytes (red blood cells, RBCs) [1][2] have shown that freezing biomaterials can be of significant clinical importance. Our experience with RBCs has shown that the formation of ice attendant to freezing can occur in two ways. Ice can form either outside cells only, or both inside and outside the cells. Experiments have shown that the presence of ice within a RBC suspended in a noncryophylactic medium usually results in cell destruction. Thus, if a freezing technique is to be of any clinical value, it must avoid the formation of intracellular ice. It follows, then, that the mechanisms of intracellular ice nucleation are of major importance in the freezing of human RBCs.

There are two general mechanisms of ice nucleation; (1) homogeneous nucleation (commonly referred to as spontaneous crystallization) in which molecules in an existing liquid phase α come together to form spontaneously a cluster of molecules in a solid phase β, and (2) heterogeneous nucleation in which the nucleation process is initiated by the presence of a catalyst, such as a foreign particle, container wall, or crevice.

Gibbs [2] laid the groundwork of homogeneous nucleation theory, and Volmer [3] utilized Gibbs' analysis to develop a kinetic homogeneous nucleation theory. Basically, as the temperature of a liquid phase is reduced to its freezing temperature, small particles of solid phase called embryos are constantly being formed, but because these embryos are unstable, they are quickly broken up. As the liquid phase is further supercooled, the number and size of these unstable embryos increases. When the temperature of the supercooled liquid reaches a particular value, the embryos reach a critical size and become metastable. The metastability of these special embryos, called nuclei, is characterized by the condition that the derivative of the Helmholtz free energy of formation of the embryo with respect to its radius vanishes. As a result, the nuclei (embryos with radii greater than or equal to the critical radius) will not disappear but instead will grow and form permanent clusters of solid phase. That is, the rate of embryo formation now exceeds the rate of embryo destruction. This nucleation condition marks the onset of freezing.

[1] Present address: Cryogenic Technology, Inc., Waltham, Mass.
[2] Numbers in brackets designate References at end of paper.

Contributed by the Heat Transfer Division for publication in the JOURNAL OF HEAT TRANSFER. Manuscript received by the Heat Transfer Division November 22, 1974. Paper No. 75-HT-DDD.

Becker and Doring [4] have improved Volmer's theory by taking into consideration the forward and backward reaction rates and have obtained an expression for the net nucleation rate. Turnbull and Fisher [5] have incorporated into the expression for the nucleation rate derived by Becker and Doring the contribution of the free energy of activation for motion of a liquid molecule across the embryo interface. A thorough discussion of the development of homogeneous nucleation is presented in references [6–8].

Turnbull [9] first looked at heterogeneous nucleation on a flat surface, in a conical cavity, and in a cylindrical cavity. Dufour and Defay [10] and later Fletcher [11] studied heterogeneous nucleation due to impurities or foreign particles in a liquid phase α. The effect of a flat surface or a foreign particle adjacent to an embryo is to reduce the value of the Helmholtz free energy of formation of an embryo of a given radius. Consequently, in heterogeneous nucleation it is possible to form nuclei at higher temperatures than in the case of homogeneous nucleation. We would expect, then, that in most physical and biological systems, heterogeneous nucleation will more likely occur instead of homogeneous nucleation; however, it is possible that both mechanisms may occur in RBCs.

It is the purpose of this paper to present an appropriate thermodynamic model which will predict the temperature for intracellular ice formation in RBCs as a function of cooling rate. Newly developed relationships describing the kinetics of water loss from the RBCs during cooling will be coupled with a derived integral expression for the net nucleation rate. For homogeneous nucleation, this integral expression relates the nucleation temperature to the nucleation rate, the volume of intracellular water, and the number of nuclei present inside the RBC. For heterogeneous nucleation the expression relates the nucleation temperature to the nucleation rate, the total surface area of catalysts present inside the RBC, and the number of nuclei adjacent to the catalysts present inside the RBC.

A parametric study of these two mechanisms was performed in the hope that the kinetics of the nucleation process might be better understood, at least for RBCs. The results show that heterogeneous nucleation is the more likely mechanism and that depending on the catalyst size and contact angle selected, the general trend predicted by the theory is in agreement with the trend of available experimental data. The results also show that the catalyst radius for heterogeneous nucleation that best correlates with experimental data is typical of the characteristic dimension of a hemoglobin molecule or a group of hemoglobin molecules.

Rate of Nucleation

Homogeneous Nucleation. Homogeneous nucleation will be initiated in a liquid when embryos of critical radius (nuclei) are formed. If J is the net rate of formation of nuclei per unit volume in a liquid phase of volume V^α, the number of nuclei formed during the time interval $t_f - t_0$ is

$$\int_{t_0}^{t_f} JV^\alpha dt = N(r_c)V^\alpha. \tag{1}$$

If the system is cooled at a constant rate

$$B = dT/dt = \text{constant}, \tag{2}$$

and equation (1) can be rewritten in the form

$$\frac{1}{B}\int_{T_0}^{T_f} JV^\alpha dT = N(r_c)V^\alpha \tag{3}$$

where T_f is the nucleation temperature at which freezing commences. The left-hand side of equation (3) represents the number of nuclei formed by collision processes, and the right-hand side represents the equilibrium number of nuclei present at the temperature and volume of the system. Homogeneous nucleation occurs when equation (3) is satisfied.

Turnbull and Fisher [5] have shown that for homogeneous nucleation the net rate of formation of embryos is given by

$$J = n_\gamma{}^\alpha N_A\left[\frac{KT}{h}\right]\frac{\Lambda\Omega_c}{g^{2/3}}\left[\frac{\Gamma}{9\pi}\right]^{1/2}\exp[-(\Delta f_A + \Delta F_c)/KT] \tag{4}$$

where the parameter Γ is proportional to the Helmholtz free energy of formation (per unit area) of the interface separating the solid

Nomenclature

B = cooling rate, °K/min
b = permeability temperature coefficient, $(°K)^{-1}$
F = Helmholtz free energy, erg
g = number of molecules contained in a nucleus, molecules/nucleus
h = Planck's constant, erg-s
h_{TP} = heat of reaction at constant T and P, erg/mole
J = homogeneous nucleation rate, nuclei/cm^3-s
J' = heterogeneous nucleation rate, nuclei/cm^2-s
K = Boltzmann constant, erg/°K
k = permeability of cell membrane, moles$^2/\mu^5$-atm-min
M = molecular weight
m = cosine of contact angle
N = number of embryos per unit volume, embryos/cm^3
N_A = Avogadro's number, molecules/mole
N_I' = number of impurities
N_S = number of embryos
n = number of moles
P = absolute pressure, dynes/cm^2
q = dimensionless constant
R = universal gas constant, erg/mole °K
r = radius, cm
s = shape factor
T = absolute temperature, °K
T_g = permeability reference temperature, °K
t = time, s
V = volume, cm^3
v = specific molar volume, cm^3/mole
x = molar fraction
z = ratio of catalyst radius to critical radius
Γ = constant in expansion of ΔF
ΔF = Helmholtz free energy of formation, erg
Δf_A = activation energy, erg
ΔT_s = degree of supercooling, °K
η = viscosity, poise
θ = contact angle, radian
Λ = number of molecules of α phase adjacent to nucleus per unit surface area, molecules/cm^2
ν = osmolality, m0sm/l
σ = surface tension, dyne/cm
ϕ = osmotic coefficient
Ω = surface area, cm^2

Subscripts

c = critical embryo
f = freezing state
I = catalyst
0 = initial state
RBC = red blood cell
s = solutes
γ = solvent; species; component

Superscripts

I = catalyst
in = intracellular
out = extracellular
α = liquid phase
β = solid phase

and liquid phases, and its value will depend upon the configuration of the interface. The term Ω_c is the surface area of the embryo exposed to the liquid phase and the term g represents the number of molecules contained within a nucleus. For a nucleus

$$\Gamma = 9(v_\gamma^\beta)^2 g^{4/3} s\sigma / KT\Omega_c^2 \tag{5}$$

where s is the shape factor and is equal to 4π for a spherical nucleus and 20.78 for a hexagonal nucleus. The right-hand side of equation (3), the equilibrium number of nuclei present at the temperature and volume of the system, is given by [12]

$$N(r_c)V^\alpha = N_A n_\gamma^\alpha \exp(-\Delta F_c / KT_f). \tag{6}$$

Substituting equations (4), (5), and (6) into equation (3), we obtain

$$\frac{1}{B}\int_{T_0}^{T_f} (n_\gamma^{\alpha\,\mathrm{in}})^2 \Lambda v_\gamma^\beta v_\gamma^\alpha \frac{KT}{h}(s\sigma/\pi KT)^{1/2} \times \exp[-(\Delta f_A + \Delta F_c)/KT]dT = n_\gamma^\alpha \exp(-\Delta F_c/KT_f). \tag{7}$$

The quantity ΔF_c appearing in equation (7) is the Helmholtz free energy of formation of a nucleus and is derived in detail in [13].

$$\Delta F_c = s\sigma r_c^2/3 \tag{8}$$

The quantity Δf_A appearing in equation (7) is the activation energy for diffusion of a molecule in the liquid phase to the surface of the nucleus. It has been suggested [14] that because of certain similarities between this diffusion process and viscous flow, the activation energy may be related to the viscosity of the liquid phase.

$$\Delta f_A = KT \ln\left[\frac{\eta_\gamma v_\gamma^\alpha}{hN_A}\right]. \tag{9}$$

Heterogeneous Nucleation. The process of heterogeneous nucleation is similar to homogeneous nucleation except that the nucleation occurs on the surface of impurities in the liquid phase rather than within the volume of the liquid phase itself. If J' is the net rate of formation of nuclei per unit surface area of impurity in a liquid phase of volume V^α with N_I' dispersed impurities of surface area Ω_I, the number of nuclei formed during the time interval $t_f - t_0$ is

$$\int_{t_0}^{t_f} J' N_I' \Omega_I dt = N_S'(r_c). \tag{10}$$

Again, if the suspension is cooled at a constant rate B, equation (10) becomes

$$\frac{1}{B}\int_{T_0}^{T_f} J' N_I' \Omega_I dT = N_S'(r_c). \tag{11}$$

The left-hand side of equation (11) represents the number of nuclei formed on the impurity surface by collision processes, and the right-hand side represents the equilibrium number of nuclei present at the temperature and impurity concentration of the system. Heterogeneous nucleation occurs when equation (11) is satisfied.

Again Turnbull and Fisher [5] have shown that for heterogeneous nucleation the net rate of formation of nuclei per unit surface area of impurity is given by

$$J' = \Lambda^2 \left(\frac{KT}{h}\right)\frac{\Omega_c}{g^{2/3}}\left[\frac{\psi}{9\pi}\right]^{1/2} \exp[-(\Delta f_A + \Delta F_c')/KT] \tag{12}$$

where the parameter ψ is proportional to the Helmholtz free energy of formation (per unit area) of the interface separating the liquid and solid phases and is given by

$$\psi = \frac{2\pi\sigma}{KT} f(m, z)[3v_\gamma^\beta/\pi h(m, z)]^{2/3} \tag{13}$$

where

$$h(m, z) = 2 + 3\left[\frac{1 - zm}{q}\right] - \left[\frac{1 - zm}{q}\right]^3 - z^3\left[2 - 3\left[\frac{z - m}{q}\right] + \left[\frac{z - m}{q}\right]^3\right] \tag{14}$$

and as shown in [11]

$$f(m, z) = 1 + \left[\frac{1 - mz}{q}\right]^3 + z^3\left[2 - 3\left[\frac{z - m}{q}\right] + \left[\frac{z - m}{q}\right]^3\right] + 3mz^2\left[\frac{z - m}{q} - 1\right] \tag{15}$$

where

$$q = (1 + z^2 - 2mz)^{1/2}. \tag{16}$$

The independent parameters m and z are the cosine of the contact angle formed between the nucleus and impurity and the ratio of the radius of the impurity to the radius of the nucleus, respectively. The right-hand side of equation (10), the equilibrium number of nuclei present at the temperature and impurity concentration of the system, is given in [12].

$$N_S'(r_c) = \Lambda N_I' \Omega_I \exp(-\Delta F_c'/KT) \tag{17}$$

The quantity $\Delta F'_c$ appearing in equations (12) and (17) is the Helmholtz free energy of formation of a spherical embryo of critical radius in contact with a spherical impurity and is derived in detail in [13].

$$\Delta F_c' = 2\pi\sigma r_c^2 f(m, z) \tag{18}$$

Notice that for the case of $r_I = 0$, i.e., no catalyst is present, equation (18) reduces to equation (8) which is the result for homogeneous nucleation. The quantity Δf_A appearing in equation (12) has already been defined in equation (9). Substituting equations (12), (13), and (17) into equation (11), we obtain after considerable algebraic manipulation

$$\frac{1}{B}\int_{T_0}^{T_f} \Lambda^2 \frac{KT}{h}\frac{2[1 + (\frac{1 - zm}{q})]}{h(m, z)} v_\gamma^\beta \left[\frac{2\sigma f(m, z)}{KT}\right]^{1/2} N_I'\Omega_I \times \exp[-(\Delta f_A + \Delta F_c')/KT]dT = \Lambda N_I'\Omega_I \exp(-\Delta F_c'/KT_f). \tag{19}$$

For both types of nucleation the freezing temperature is determined by the value of T_f that satisfies equation (7) or equation (19) depending upon the nucleation mechanism. Because of the complex temperature dependence of the various terms appearing in the integrals on the left-hand sides of these equations, it is not possible to obtain closed form solutions. Instead, it is necessary to use a numerical method which involves selecting a value of T_f and evaluating the left-hand and right-hand sides of equations (7) or (19) independently. If the two sides are not equal, a new value of T_f is selected. The process is repeated until the two sides of the equations agree. Note that equations (7) and (19) are general in that they can be applied to open systems for which the number of molecules of the liquid phase vary with time in both the homogeneous and heterogeneous cases and the number of impurities vary with time in the heterogeneous case.

Red Blood Cell Model

The physical dimensions and internal composition of the RBCs are given in references [15, 16]. It is assumed the cell membrane is permeable only to water and impermeable to solutes; consequently, the hemoglobin and dissociated electrolytes are not able to leave the cell during the cooling and thawing processes. The permeability of the membrane to water is assumed to be of the form [13]

$$k = 1.85 \times 10^{-15} \exp[335.174/\nu - 26.286 + b(T - T_g)] \tag{20}$$

where $T_g = 293°\mathrm{K}$ in the present case.

The foregoing expression for the permeability of water takes into consideration not only the temperature of the system but also the osmolality of the extracellular solution. Note that the permeability decreases as the temperature decreases. During the freezing process, ice will form preferentially outside the cells due to the minute temperature gradients responsible for conduction heat

transfer from the cells to the boundaries of the suspending medium in contact with the coolant. Because of the presence of extracellular ice, a chemical potential difference will exist between extracellular and intracellular solutions. Intracellular water will begin to flow out of the cells in order to reduce this difference and maintain equilibrium. As water flows out of the cells, cell volume decreases resulting in an inward displacement of the cell membrane. Since intracellular proteins such as hemoglobin cannot penetrate healthy membranes, they accumulate along the inner surface of the membrane which produces a spatial concentration gradient of protein within the cell. In effect, the moving membrane sweeps these molecules out of the intracellular solution like so many fish caught in a net. As the temperature is reduced further, the membrane permeability to water decreases, and the presence of the randomly stacked layers of protein adjacent to the inner wall of the cell membrane further increases the resistance of the membrane to water flow. The decrease in mobility of water across the cell membrane causes the concentration of solutes within the cell to increase less rapidly than the concentration outside the cell. Since both the extracellular and intracellular media are at the same temperature, the intracellular medium becomes supercooled. As a result, conditions favorable to intracellular nucleation, either homogeneous or heterogeneous, soon develop inside the cell. Clearly, the time required for these conditions to develop will depend upon the cooling rate and the cell characteristics.

Mazur [17] first studied the volume change of RBCs due to water loss during the cooling process. A later study [13] which represents an extension of Mazur's model reveals that the osmolality of the extracellular solution as well as the degree of supercooling can significantly alter the volumetric changes of RBCs during the cooling process.

Three coupled equations describe the response of the cell to changes in temperature:

1 Rate equation:

$$\frac{dn_\gamma^{\alpha \text{in}}}{dt} = -\frac{k\Omega_{\text{RBC}}RT\phi}{B} \ln\left(x_\gamma^{\alpha \text{in}}/x_\gamma^{\alpha \text{out}}\right) \tag{21}$$

2 Mass conservation equation:

$$\frac{dn_\gamma^{\alpha \text{in}}}{dT} + \frac{dn_\gamma^{\alpha \text{out}}}{dT} + \frac{dn_\gamma^{\beta \text{out}}}{dT} = 0 \tag{22}$$

3 Equilibrium equation (external medium):

$$\frac{dn_\gamma^{\beta \text{out}}}{dT} = -\frac{dn_\gamma^{\alpha \text{in}}}{dT} - h_{TP}[n_\gamma^{\alpha \text{out}} + 2n_s^{\text{out}}]/2RT^2 n_s^{\text{out}}\left[\frac{\phi}{n_\gamma^{\alpha \text{out}}} - \frac{\frac{\partial \phi}{\partial x_s^{\text{out}}} \ln x_\gamma^{\alpha \text{out}}}{n_\gamma^{\alpha \text{out}} + 2n_s^{\text{out}}}\right] \tag{23}$$

The solutions of these equations do not predict the temperature at which intracellular ice may appear but instead show the behavior of the molar concentration of the intracellular solution as a function of the temperature of the system consisting of the cell and its suspension. To determine the intracellular freezing temperature, it is necessary to combine equations (21), (22), and (23) with either equation (7) or equation (19) depending on the nucleation mechanism.

Results

For the case of homogeneous nucleation, we have used this technique to determine the intracellular freezing temperature in RBCs experiencing different cooling rates. These results are presented in Fig. 1. The cell volumes used in the calculations varied from $30\mu^3$ to $200\mu^3$ which corresponds to 99.99 percent of the Gaussian distribution of volumes of human RBCs. The nucleation temperatures only differed a degree in the volume range of $30\mu^3$–$200\mu^3$ at a particular cooling rate. Thus, the dependence of the homogeneous nucleation temperature on RBC volume is quite weak. Notice that

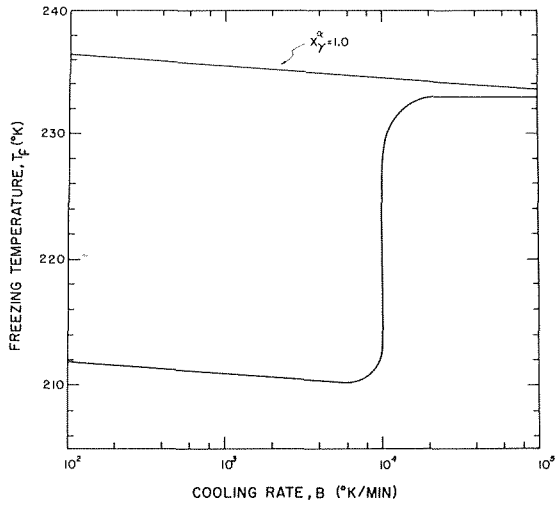

Fig. 1 Homogeneous freezing temperature of red blood cells cooled at constant rates

there exists a sharp distinction between the nucleation temperatures at cooling rates less than 10,000°K/min and larger than 10,000°K/min. The average homogeneous nucleation temperature is on the order of 210–212°K for the lower cooling rate and on the order of 230–233°K for the higher cooling rates. The critical radius of the nuclei corresponding to these nucleation temperatures and cooling rates is on the order of 10Å.

As a comparison, the freezing temperature for homogeneous nucleation in a RBC composed only of pure water with a volume between $18.95\mu^3$ and $126.30\mu^3$ (i.e., 63.15 percent of the normal RBC volume) is evaluated and is represented by the solid straight line in Fig. 1, i.e., the case for $x_\gamma^\alpha = 1.0$. The homogeneous freezing temperature increases as the cooling rate decreases which is evident from the form of equation (3). For cooling rates larger than 10,000°K/min, the two analytical curves are separated only by a small difference which is due to the initial electrolyte concentration in a RBC. However, for cooling rates smaller than 10,000°K/min, there is a large difference between the two analytical curves due to the formation of a solid eutectic solution at the smaller cooling rates.

The evaluation of the freezing temperature for the case of heterogeneous nucleation is a bit more involved than the homogeneous case because of the complex way in which the impurity characteristics affect the kinetics. For these calculations we have assumed the impurities on which nucleation occurs to be spheres with radii of 32 Å and a number density of 32×10^7 per cell. Both of these characteristics are typical of intracellular proteins. We also need to establish the contact angle between the embryo and impurity on which the embryos form. Since no information is available about this contact angle for typical biomaterials, we have calculated the freezing temperature, T_f, for various contact angles between 0 and π radians (or alternatively the parameter m, which is the cosine of the contact angle, was varied between -1.0 and $+1.0$).

The results of these calculations are presented as a function of cooling rate in Fig. 2 for a RBC with the physical dimensions noted previously and an impurity of radius 32Å. Notice that for a given value of m, the temperature for heterogeneous nucleation is a strong function of cooling rate within a narrow range of cooling rates which we have termed the demarcation zone. For cooling rates below the demarcation zone the nucleation temperature is low, but for cooling rates above the demarcation zone, the nucleation temperature is high. Notice also that as m increases from -1.0 to $+1.0$, the range of cooling rates that influence nucleation temperatures decreases from 9000°K/min to 2000°K/min. Also for these variations of m, the nucleation temperature at any given cooling rate increases as m increases. This behavior is due to the fact that large values of m result in large values of the critical radi-

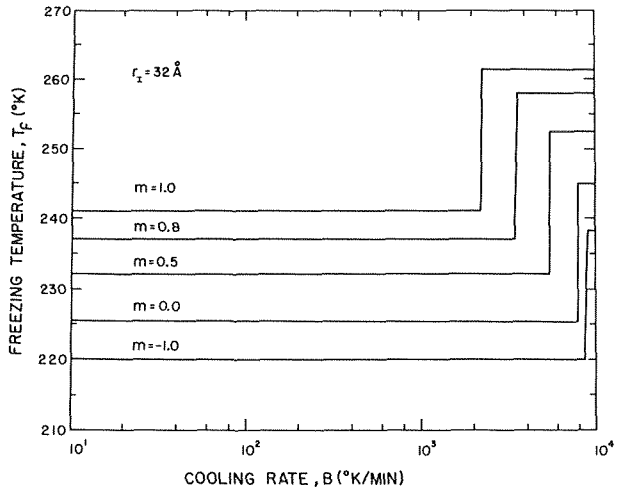

Fig. 2 Effect of contact angle on heterogeneous freezing temperatures of red blood cells cooled at constant rates

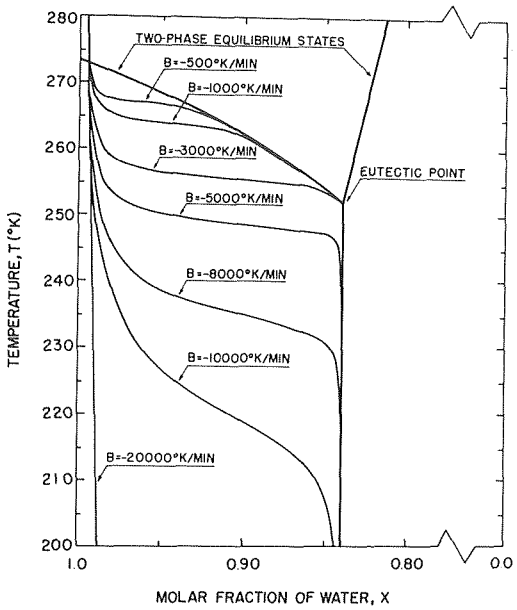

Fig. 4 Locus of states of intracellular solution of red blood cells cooled at constant rates (states of extracellular solution coincident with locus of two-phase equilibrium states)

us, which in turn lead to high nucleation temperatures. The aforementioned demarcation zone is so narrow that we can readily quantify fast and slow cooling rates for a given value of m. The results of Fig. 2 show that the nucleation temperature for slow cooling rates ranges from 220°K to 241°K while the nucleation temperature for fast cooling rates ranges from 239°K to 262°K. These values for the heterogeneous nucleation temperature are significantly higher than the corresponding values for the homogeneous nucleation temperature. In contrast to homogeneous nucleation, the freezing temperature for heterogeneous nucleation is completely independent of RBC volume. This is to be expected since the homogeneous nucleation process depends upon the volume of the liquid phase in the cell whereas the process of heterogeus nucleation depends on the number of nucleation sites in the cell. The number of these sites is sufficiently large in any healthy cell to saturate the cell with nucleation sites.

In the event that the impurities agglomerate, the nucleation rate will be markedly affected because the $\Delta F_c'$ required for the formation of a nucleus will be smaller; consequently for a particular cooling rate the freezing temperature will be higher for a larger size catalyst. To determine the effect of the packing or agglomeration of the impurity molecules, we varied the impurity radius in increments of 32Å from 32Å to 160Å and calculated the freezing temperature for a contact angle of zero radians (i.e., $m = +1.0$) which results in a critical radius equal to the radius of the impurity. The results of these calculations are shown in Fig. 3.

Notice that as the radius of the impurity increases from 32Å to 160Å, the cooling rate corresponding to the demarcation zone decreases from 2000°K/min to 200°K/min. The range of nucleation temperatures for low cooling rates varies from 241°K to 249°K, and the range of nucleation temperatures for high cooling rates varies from 262°K to 270°K. Fig. 3 also shows that because of the hyperbolic dependence of the critical radius on temperature, the heterogeneous nucleation temperature for a particular cooling rate increases as the impurity radius increases, but only up to a certain limit. Beyond this limit, the nucleation temperature is essentially independent of impurity size. This can be seen if one replots the analytical data in Fig. 3 for the freezing temperature versus impurity radius with cooling rate as the parameter (cf. Fig. 7).

The sharp demarcation between high and low cooling rates is of special interest because of its potential importance in clinical applications. The demarcation is due to the variation of intracellular water during freezing. Fig. 4 shows the molar fraction of intracellular water at various cooling rates for a typical RBC as obtained from simultaneous solutions of equations (21), (22), and (23). In all cases it is assumed that the external solution follows the equilibrium curve from 272.4°K, the normal freezing temperature of the solution, to the eutectic temperature 252.0°K. At the eutectic temperature, the remaining extracellular solution forms a solid solution such that the external medium consists of pure ice and the solid solution. Because of the resistance to water transport offered by the membrane, the intracellular medium is supercooled and nucleation may occur at temperatures below the eutectic temperature. In Fig. 4, notice that for cooling rates less than 3000°K/min, the cooling curves join the equilibrium curve at temperatures greater than the eutectic temperature, but for cooling rates larger than 3000°K/min, the cooling curves join the equilibrium curve below the eutectic temperature. It was shown in reference [13] that similar results can be obtained by holding the cooling rate constant and varying the membrane permeability; thus, it follows that a cell cooled at a high rate behaves as though it has a membrane with a low water permeability. That is, the heat transfer dominates over

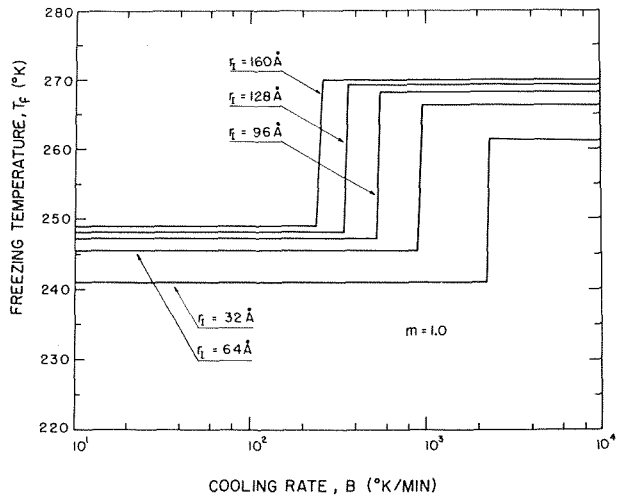

Fig. 3 Effect of catalyst radius on heterogeneous freezing temperatures of red blood cells cooled at constant rates

the mass transfer so that intracellular water is trapped inside the cell and pure ice precipitates out of the intracellular solution at a supercooled temperature. At low cooling rates, the converse is true. Mass transfer dominates over heat transfer so that a considerable portion of the intracellular water leaves the cell and a solid solution forms within the cell at a subeutectic temperature.

The existence of a sharp demarcation betweeen high and low cooling rates is in agreement with the experimental data obtained by Diller [18]. He has shown that for cooling rates larger than 850°K/min, intracellular ice is formed in 100 percent of the RBCs in the specimens, whereas for cooling rates less than 840°K/min, he was not able to detect intracellular ice by light microscopy. It is possible that the solid solution was present in these latter cases but was not detectable by his technique.

Because RBCs frequently are supercooled in clinical applications, it is worthwhile to study carefully the effect of the degree of supercooling, ΔT_s, on the heterogeneous freezing temperature of RBCs as a function of cooling rate and catalyst radius. In Fig. 5 is presented the heterogeneous freezing temperature of RBCs for supercooling of 0°K, 5°K, 8°K, 9.8°K, and 10.1°K, respectively, for a catalyst radius of 32Å and a contact angle of 0 deg. Notice that the demarcation zone is shifted to slower cooling rates for higher degrees of supercooling. This trend is in agreement with the experimental data obtained by Diller [19]. For 0°K supercooling, the demarcation zone appeared between 840°K/min and 850°K/min, for 5°K supercooling, the demarcation zone appeared between 795°K/min and 805°K/min, and for 12°K supercooling, the demarcation zone appeared between 6°K/min and 16°K/min. In order to study the effect of impurity packing as well as supercooling, the cooling rates corresponding to the demarcation zone are presented in Fig. 6 as a function of supercooling and catalyst radius along with the experimental data of Diller [19]. Again the demarcation zone cooling rate is shifted to lower values for both a larger degree of supercooling and a larger catalyst radius.

It is also possible that the kinetics of intracellular ice nucleation may be initiated by the propagation of ice crystals from the extracellular medium through the cell membrane to the intracellular medium. Mazur [17] has proposed such a mechanism based upon a porous membrane model. When ice first appears extracellularly, the membrane acts as a barrier to the penetration of ice, but as the cell suspension is cooled further, the intracellular contents supercool. Water trapped in the membrane pores nucleates with the extracellular ice acting as a catalyst. The ice then propagates through the membrane and acts as the catalyst for the heterogeneous nucleation of ice inside the cell. The relationship between the cooling velocity, freezing temperature, and catalyst radius operative in this

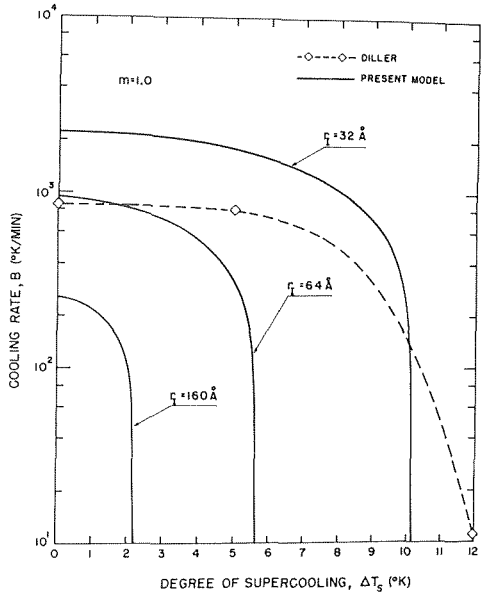

Fig. 6 Effect of catalyst radius on demarcation zone cooling rate for supercooled red blood cells

mechanism can be readily obtained from the present analysis for the RBC.

From measurements of the osmotic pressure gradient across RBC membranes [20], the number of pores in a RBC membrane can be shown to be approximately 5.96×10^4 pores/RBC. Then with an effective catalyst radius (propagating ice crystal radius) equal to the membrane pore radius and a contact angle of 0 deg ($m = +1.0$) between the ice crystal catalyst and the embryo, equation (10) can be employed with N_I' the number of pores and Ω_I the exposed surface areas of the ice crystal propagating through the pore. For a pore radius varying from 1.0Å to 32.0Å the resulting heterogeneous nucleation temperatures for the case of zero supercooling are shown in Fig. 7 together with the results of heterogeneous nucleation for r_I = 32Å previously shown in Fig. 3. The top solid line corresponds to the intracellular nucleation of pure ice whereas the bottom solid line corresponds to the nucleation of a solid solution of pure ice and eutectic solid inside the cell at subeutectic temperatures.

Note that the results for heterogeneous nucleation by ice propagation through the cell membrane are indistinguishable from the

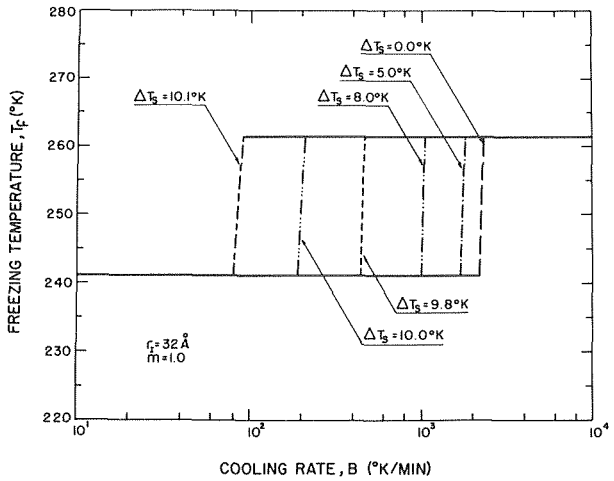

Fig. 5 Effect of supercooling on heterogeneous freezing temperatures of red blood cells cooled at constant rates

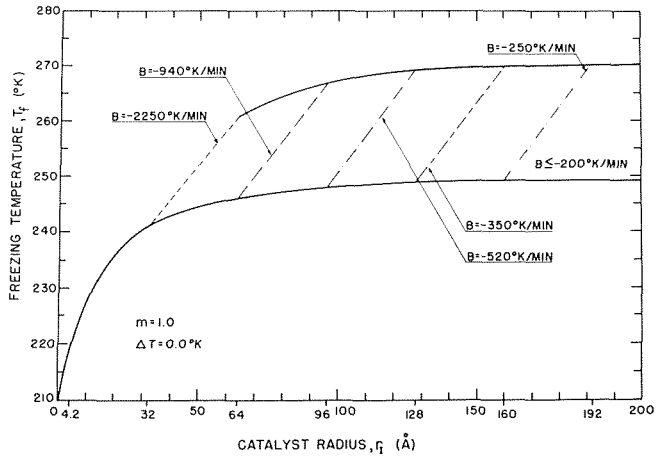

Fig. 7 Effect of catalyst radius on heterogeneous freezing temperatures of red blood cells cooled at constant rates for both heterogeneous nucleation mechanisms

results of heterogeneous nucleation on the surface of a spherical impurity because the intracellular medium in both cases is saturated with catalyst on which ice embryos can form. Thus, the freezing temperature in effect becomes a function of catalyst radius only. Note also in Fig. 7 that as the catalyst radius approaches zero, the heterogeneous freezing temperature approaches the freezing temperature for homogeneous nucleation.

Conclusions

The results of the present study reveal that heterogeneous nucleation is a possible mechanism in RBCs. These cells contain catalyst of sufficient size and in sufficient numbers, either singly or in groups, to trigger the nucleation process. Available experimental data are not adequate to identify the nature of the catalyst, but several possibilities exist. Of course, it is also possible for the intracellular medium to nucleate even in the absence of a catalyst. However, for this homogeneous nucleation process, the freezing temperature is approximately 30°K lower than for the heterogeneous case.

Both heterogeneous and homogeneous nucleation are divided into two distinct regions—low cooling rates and high cooling rates—separated by a demarcation zone. High freezing temperatures are typical of high cooling rates and low freezing temperatures are typical of low cooling rates. For heterogeneous nucleation, the demarcation zone shifts to lower cooling rates as the size of the catalyst increases. Thus, the larger the catalyst, the higher will be the freezing temperature at a given cooling rate. All of these results of the analysis imply that intracellular freezing of human RBCs is probably due to heterogeneous nucleation triggered by some catalyst.

The analysis also shows that if the extracellular medium is allowed to supercool, the probability of finding intracellular ice in RBCs will increase since the demarcation zone shifts to lower cooling rates as the degree of supercooling increases. Furthermore, the greater the degree of supercooling, the more sensitive the RBC freezing temperature becomes to intracellular ice formation. That is, when the degree of supercooling is high, a shift in supercooling of a few tenths of a degree in temperature can shift the demarcation zone by an order of magnitude of more. The analytical results are in agreement with past experimental data and clinical experience. It follows, then, that supercooling should be minimized in clinical freezing if the lethal effects of intracellular ice are to be avoided.

Acknowledgments

This work was supported in part by USPHS Grant 1 PO1 HL14322-03 from NHLI; and Fundacao de Amparo a Pesquisa do Estado do Sao Paulo and Escola Politecnica da Universidade de Sao Paulo, Brazil.

References

1 Huggins, C. E., "Practical Preservation of Blood by Freezing," in *Red Cell Freezing*, A technical Workshop Presented by Committee on Workshops of the American Association of Blood Banks, 1973, pp. 31–53.

2 Gibbs, J. W., *Scientific Papers*, Vol. 1, Dover, New York, 1961, pp. 219–331.

3 Volmer, M., "Zum Problem des Kristall wachstums," *Z. Physik, Chem.*, Vol. 102, 1922, pp. 267–275.

4 Becker, R., and Doring, W., "Kinetische Behandlung der Keimbildung in Übersäthgten Dämpfen," *Ann. Physik.*, Vol. 24, 1935, pp. 719–752.

5 Turnbull, D., and Fisher, J. C., "Rate of Nucleation in Condensed Systems," *J. Chem. Phys.*, Vol. 17, 1949, pp. 71–73.

6 Dufour, L., and Defay, R., *Thermodynamics of Clouds*, Academic Press, New York, 1963.

7 Uhlmann, R., and Chalmers, B., "The Energetics of Nucleation," *Industrial and Engineering Chemistry*, Vol. 57, 1965, pp. 19–31.

8 Parker, R. L., "Crystal Growth Mechanisms: Energetics, Kinetics, and Transport," *Solid State Physics*, Vol. 25, Turnbull, ed., 1970, pp. 152–301.

9 Turnbull, D., "Kinetics of Heterogeneous Nucleation," *J. Chem. Phys.*, Vol. 18, 1950, pp. 198–203.

10 Dufour, L., and Defay, R., "Sur la formation des germes de condensation et de solidification autour d'un noyay solide insoluble," *Tellus*, Vol. 5, 1953, pp. 293–301.

11 Fletcher, N. H., "Size Effect in Heterogeneous Nucleation," *J. Chem. Phys.*, Vol. 29, 1958, pp. 572–576.

12 Fisher. J. C., Hollomon, J. H., and Turnbull, D., "Nucleation," *J. Appl. Phys.*, Vol. 19, 1948, pp. 775–784.

13 Silvares, O. M., "A Thermodynamic Model of Water and Ion Transport across Cell Membranes during Freezing and Thawing: The Human Erythrocyte," PhD thesis, Massachusetts Institute of Technology, Sept. 1974.

14 Glasstone, S., Laidler, K. J., and Eyring, H., *The Theory of Rate Processes*, McGraw-Hill, New York, 1941.

15 Canham, P. B., and Burton, A. C., "Distribution of Size and Shape in Populations of Normal Human Red Cells," *Circulation Research*, Vol. 22, 1968, pp. 405–422.

16 Wintrobe, M. M., *Clinical Hematology*, Lea and Febiger, Philadelphia, 1967, pp. 106–107.

17 Mazur, P., "Physical and Chemical Bases of Injury in Single-Celled Microorganisms Subjected to Freezing and Thawing," *Cryobiology*, H. T. Meryman, ed., Academic Press, New York, 1966, pp. 213–315.

18 Diller, K. R., "A Microscopic Investigation of Intracellular Ice Formation in Frozen Human Erythrocytes," ScD thesis, Massachusetts Institute of Technology, June 1972.

19 Diller, K. R., "Intracellular Freezing: Effect of Extracellular Supercooling," to be published in *Cryobiology*.

20 Paganelli, C. V., and Solomon, A. K., "The Rate of Exchange of Tritiated Water Across the Human Red Cell Membrane," *Journal of General Physiology*, Vol. 41, 1957, pp. 259–277.